

Chip-Interleaved Block-Spread Code Division Multiple Access

Shengli Zhou, *Student Member, IEEE*, Georgios B. Giannakis, *Fellow, IEEE*, and Christophe Le Martret

Abstract—A novel multiuser-interference (MUI)-free code division multiple access (CDMA) transceiver for frequency-selective multipath channels is developed in this paper. Relying on chip-interleaving and zero padded transmissions, orthogonality among different users' spreading codes is maintained at the receiver even after frequency-selective propagation. As a result, deterministic multiuser separation with low-complexity code-matched filtering becomes possible without loss of maximum likelihood optimality. In addition to MUI-free reception, the proposed system guarantees channel-irrespective symbol detection and achieves high bandwidth efficiency by increasing the symbol block size. Filling the zero-gaps with known symbols allows for perfectly constant modulus transmissions. Important variants of the proposed transceivers are derived to include cyclic prefixed transmissions and various redundant or nonredundant precoding alternatives. (Semi-) blind channel estimation algorithms are also discussed. Simulation results demonstrate improved performance of the proposed system relative to competing alternatives.

Index Terms—Block spreading, channel estimation, chip interleaving, code division multiple access (CDMA), multipath, multiuser interference.

I. INTRODUCTION

RELYING on orthogonal spreading codes, code division multiple access (CDMA) systems enable simultaneous transmissions from multiple users over the same bandwidth and time duration. However, when the chip rate increases, the underlying multipath channel becomes frequency selective; it introduces inter chip interference (ICI), and thus destroys code orthogonality at the receiver. The latter gives rise to multiuser interference (MUI). To suppress MUI, various multiuser detectors are available [26], e.g., the linear decorrelating or zero forcing (ZF), the minimum mean square error (MMSE), as well as the nonlinear decision feedback (DF) and maximum likelihood (ML) receivers. However, these schemes require knowledge of the multipath channels for all users and/or

suppress MUI statistically (except for the ZF option) even with exact channel state information (CSI). In addition to increased complexity that comes with multichannel estimation and multiuser detection, there even exist frequency-selective channels preventing symbol detection no matter what receiver is used (see [10] for illuminating counter-examples).

To remove MUI deterministically *regardless* of the underlying multipath channels, several alternatives have been proposed recently. Those include the orthogonal frequency division multiple access (OFDMA) [22] (and generalizations [25]), where complex exponentials are utilized as information-bearing subcarriers that retain their orthogonality when passing through multipath channels. However, when the channels have nulls (or deep fades) on some subcarriers, the information symbols on those subcarriers will be lost. Therefore, OFDMA-like transceivers require extra diversity (such as frequency hopping or channel coding) to ameliorate fading effects. To guarantee channel-irrespective MUI-free reception and symbol detection, a mutually-orthogonal usercode-receiver (AMOUR) system was proposed in [11]. Subsequently, a generalized multi-carrier (GMC) CDMA was developed in [10], [27] that also unifies many existing schemes. However, similar to all multicarrier systems, AMOUR transmissions are not constant-modulus (C-M) in general, even though a special code design exhibits C-M, and will turn out to fall under the system designs developed herein. AMOUR codes are generally complex valued and bandwidth efficiency drops by 50% if real codes are to be designed from complex ones [27]. To maintain C-M at the transmitter and facilitate low-complexity receivers for MUI-free reception, the so-called shift orthogonal codes (which are not only orthogonal to each other but also to their shifted versions) were proposed in [15] and [16]. However, to maintain shift orthogonality, a 50% bandwidth efficiency penalty is paid for both the real and the complex codes in [15] and [16].

In this paper, we develop novel MUI-free CDMA transceivers based on a specific block-spreading operation, which can be viewed as (and is implemented by) symbol-spreading followed by chip interleaving. The resulting so-called chip interleaved block spread (CIBS) transceivers are applicable to both uplink and downlink scenarios. Thanks to chip-interleaving and zero padding at the transmitter, mutual orthogonality between different users' codes is preserved even after multipath propagation, which enables deterministic multiuser separation through low-complexity code-matched filtering without loss of maximum likelihood optimality. Consequently, multiuser detection is successfully converted to a set of equivalent single-user equalization problems (Section III). In addition to

Paper approved by W. A. Krzymien, the Editor for Multicarrier and Spread Spectrum Systems of the IEEE Communications Society. Manuscript received August 31, 2000; revised June 9, 2001. This work was supported by the National Science Foundation under Wireless Initiative Grant 99-79443 and NSF Grant 0105612. This paper was presented in part at the 38th Allerton Conference, University of Illinois at U-C, Monticello, IL, October 4–6, 2000, and at the 35th Conference on Information Sciences and Systems, the Johns Hopkins University, Baltimore, March 21–23, 2001.

S. Zhou and G. B. Giannakis are with the Department of Electrical and Computer Engineering, University of Minnesota, Minneapolis, MN 55455 USA (e-mail: szhou@ece.umn.edu; georgios@ece.umn.edu).

C. Le Martret was with the Department of Electrical and Computer Engineering, University of Minnesota, Minneapolis, MN 55455 USA, on leave from the Centre d'Électronique de L'Armement (CELAR), 35170 Bruz, France (e-mail: c.lemartret@wanadoo.fr).

Publisher Item Identifier S 0090-6778(02)01360-0.

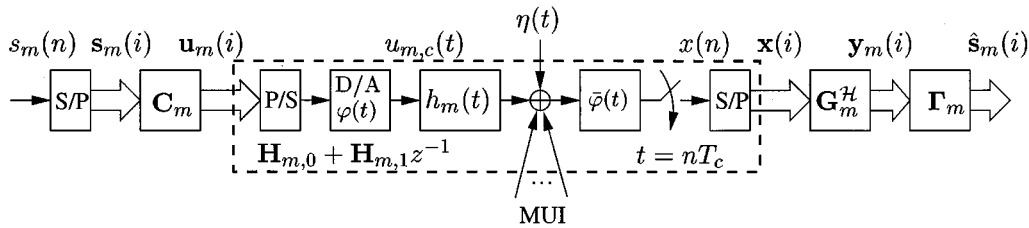


Fig. 1. Continuous and discrete-time equivalent system model.

MUI-free reception, channel-irrespective symbol detection is also guaranteed. Since the only requirement is mutual orthogonality among users' codes, the code design is very flexible and enables fast algorithms at the receiver. By increasing the symbol block size, the proposed system achieves high bandwidth efficiency. Perfectly constant modulus transmissions become available by filling the zero gaps with known symbols. Variants of the proposed transceivers are also developed in Section IV to include cyclic prefixed (CP) transmissions as well as various (redundant or nonredundant) precoded and loaded transmissions. Transforming the multiple-input multiple-output (MIMO) channel to an equivalent set of parallel single-input single-output (SISO) channels implies that the receiver can employ various training-based or (semi-) blind channel estimators developed for single user systems (Section V). Simulations are then performed in Section VI and concluding remarks are drawn in Section VII.

Notation: Bold upper (lower) letters denote matrices (column vectors); $(\cdot)^T$ and $(\cdot)^H$ denote transpose and Hermitian transpose, respectively; $\delta(\cdot)$ and \otimes stand for Kronecker's delta and Kronecker product, respectively. $E\{\cdot\}$ for expectation, $\lceil \cdot \rceil$ for integer ceiling; \mathbf{I}_K denotes the identity matrix of size K ; $\mathbf{0}_{M \times N}$ ($\mathbf{1}_{M \times N}$) denotes an all-zero (all-one) matrix with size $M \times N$; and, \mathbf{F}_K denotes a $K \times K$ FFT matrix with $(p+1, q+1)$ th entry $(1/\sqrt{K})e^{-j2\pi pq}$, $\forall p, q \in [0, K-1]$.

II. SYSTEM MODELING

The block diagram in Fig. 1 describes a CDMA system model in either uplink or downlink operation, where only one user (the m th user out of a maximum M users) is shown. Unlike traditional spreading which is performed over a *single symbol*, we here use block spreading that operates on a *block of symbols*; block spreading has also been used in, e.g., [27], [11], [15], and [16]. Specifically, the information stream of the m th user $s_m(n)$ is first parsed into blocks¹ of length K : $\mathbf{s}_m(i) := [s_m(iK), s_m(iK+1), \dots, s_m(iK+K-1)]^T$, and then block spread by a $P \times K$ spreading matrix \mathbf{C}_m to obtain the $P \times 1$ output vector $\mathbf{u}_m(i) := \mathbf{C}_m \mathbf{s}_m(i)$. Viewing each column of \mathbf{C}_m (the $(k+1)$ -st column denoted by $\tilde{\mathbf{c}}_{m,k}$) as a separate spreading code for user m , the block spreading can be thought of as a multicode transmitter (K codes per user), since we can write the transmitted block as: $\mathbf{u}_m(i) = \sum_{k=0}^{K-1} \tilde{\mathbf{c}}_{m,k} s_m(iK+k)$ [28].

After parallel to serial (P/S) conversion of $\mathbf{u}_m(i)$, the m th user's coded chip sequence $u_m(n)$ is pulse shaped to the corresponding continuous time signal

$u_m(t) = \sum_{n=-\infty}^{\infty} u_m(n)\varphi(t - nT_c)$, where T_c is the chip period and $\varphi(t)$ is the chip pulse. The m th user's transmitted signal $u_m(t)$ propagates through a (possibly *unknown*) channel $g_m(t)$ and is filtered by the receive filter $\tilde{\varphi}(t)$ that is matched to $\varphi(t)$. Let $R_{\varphi\tilde{\varphi}}(t)$ be the convolution of transmit- with receive-filters. With \star denoting convolution, let $h_m(l) := (\varphi \star g_m \star \tilde{\varphi})(t)|_{t=lT_c} = \int_{-\infty}^{\infty} g_m(\tau) R_{\varphi\tilde{\varphi}}(lT_c - \tau) d\tau$ be the chip-sampled discrete time equivalent FIR channel corresponding to the m th user. The FIR channel $h_m(l)$ of order L_m includes the m th user's asynchronism in the form of delay factors as well as transmit-receive filters and frequency-selective multipath effects. With $\eta(n) := (\eta \star \tilde{\varphi})(t)|_{t=nT_c}$ denoting sampled noise, the aggregate received sequence from all M users at the chip rate can then be written as

$$x(n) = \sum_{m=0}^{M-1} \sum_{l=0}^{L_m} h_m(l)u_m(n-l) + \eta(n). \quad (1)$$

Similar to [22], [25], [11], and [15], we here focus on a practical quasi-synchronous (QS) system in the *uplink*, where the mobile users attempt to synchronize with the base-station's pilot waveform and have a coarse common timing reference. A good example is the European 3rd Generation mobile communication system based on hybrid TDMA/CDMA (briefly denoted as T-CDMA), where multiple users per cell are allowed to transmit over the same time slot [1]. Asynchronism among users is thus limited to only a few chip intervals; the maximum asynchronism $\tau_{\max,a}$ arises between the nearest and the farthest mobile users within the cell, and can be predetermined from the radius of the cell and the adopted chip interval T_c . With $\tau_{\max,s}$ denoting maximum multipath spread, which is found using field measurements from the operational environment, the maximum channel order $L := \max_m L_m$ can be found as $L = \lceil (\tau_{\max,s} + \tau_{\max,a})/T_c \rceil$; see, e.g., [28] for some calculation examples with real channels.

The *downlink* model (from the base station to the user of interest m_0) is subsumed by the uplink (1): indeed, setting $h_m(l) = h_{m_0}(l), \forall m \in [0, M-1]$, is a special case of (1) since the latter allows for distinct user channels. The downlink transmissions are synchronous with $\tau_{\max,a} = 0$, and the maximum channel order L depends only on $\tau_{\max,s}$ through $L = \lceil \tau_{\max,s}/T_c \rceil$. In either uplink or downlink transmissions, the only channel knowledge² assumed at the transmitter is L , and we always choose block size $P \gg L$.

¹Arguments n, k, i will denote, respectively, chip, symbol, and block-of-symbols indices.

²This is in contrast with the joint transmitter and receiver optimization based approaches of, e.g., [14], [24], where the multipath characteristics of all channels are known at the transmitter.

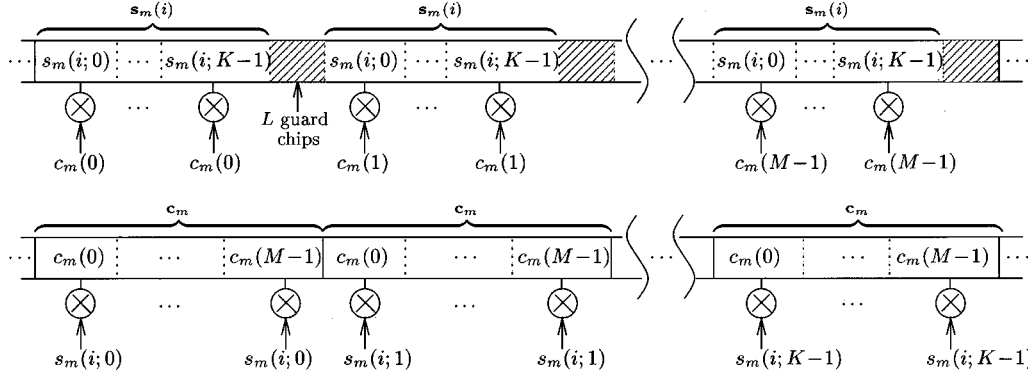


Fig. 2. Top: serial version of the i th transmitted block $\mathbf{u}_m(i) = \mathbf{C}_m \mathbf{s}_m(i)$ of length $M(K + L)$ versus the conventional CDMA transmission of K symbols, each spread with a short code of length M (bottom).

The linear multiuser separating front-end for user μ is described by the matrix \mathbf{G}_μ . Extracting the μ th user of interest from $\mathbf{x}(i)$ yields the MUI-free block

$$\mathbf{y}_\mu(i) = \mathbf{G}_\mu^H \mathbf{x}(i). \quad (2)$$

The MUI-free output $\mathbf{y}_\mu(i)$ is then equalized by *any* single user equalizer, e.g., a linear equalizer $\mathbf{\Gamma}_\mu$ will yield symbol block estimates $\hat{\mathbf{s}}_\mu(i)$

$$\hat{\mathbf{s}}_\mu(i) = \mathbf{\Gamma}_\mu \mathbf{y}_\mu(i). \quad (3)$$

Starting from the general block spreading system model described by (7) and (2), we will propose next judiciously designed transceiver pairs $\{\mathbf{C}_m, \mathbf{G}_m\}_{m=0}^{M-1}$ that enable separation of superimposed multiuser signals deterministically and guarantee detection of each user's symbols *regardless of* multipath propagation through FIR frequency-selective channels of maximum order L .

III. CIBS-CDMA TRANSCIVER DESIGN

To design transceiver pairs $\{\mathbf{C}_m, \mathbf{G}_m\}_{m=0}^{M-1}$, we start by assigning to each user a distinct short signature vector of length M denoted by $\mathbf{c}_m := [c_m(0), \dots, c_m(M-1)]^T$. These vectors are selected to be mutually orthogonal which can be formally stated as a design constraint:

d1) select code-generating vectors: $\mathbf{c}_\mu^H \mathbf{c}_m = \delta(\mu-m), \forall \mu, m \in [0, M-1]$.

Based on the orthogonal signature vectors $\{\mathbf{c}_m\}_{m=0}^{M-1}$, we next specify the block spreading matrix \mathbf{C}_m and the user-separating matrix \mathbf{G}_m .

Consider the $(K+L) \times K$ matrix $\mathbf{T}_{zp} := [\mathbf{I}_K, \mathbf{0}_{K \times L}]^T$ that we term zero-padding (ZP) matrix because, upon premultiplication with a $K \times 1$ vector, it appends L zeros. Based on \mathbf{T}_{zp} , we select our $P \times K$ user code matrices \mathbf{C}_m and correspondingly the $(K+L) \times P$ separating matrices \mathbf{G}_m as

$$\mathbf{C}_m = \mathbf{c}_m \otimes \mathbf{T}_{zp}, \quad \mathbf{G}_m = \mathbf{c}_m \otimes \mathbf{I}_{K+L} \quad (4)$$

where, using the Kronecker product definition, we have block length $P = M(K+L)$. In our subsequent derivations, we re-

peatedly use the following two identities of Kronecker products applied to matrices with matching dimensions [5]:

$$(\mathbf{A}_1 \otimes \mathbf{A}_2)^H = \mathbf{A}_1^H \otimes \mathbf{A}_2^H \quad (5)$$

$$(\mathbf{A}_1 \otimes \mathbf{A}_2)(\mathbf{A}_3 \otimes \mathbf{A}_4) = (\mathbf{A}_1 \mathbf{A}_3) \otimes (\mathbf{A}_2 \mathbf{A}_4). \quad (6)$$

Using (5) and (6), we infer that under d1) the transceiver design of (4) ensures mutual orthogonality among users: $\mathbf{C}_\mu^H \mathbf{C}_m = \delta(\mu-m) \mathbf{I}_K$ and $\mathbf{G}_\mu^H \mathbf{G}_m = \delta(\mu-m) \mathbf{I}_{K+L}$.

For the \mathbf{C}_m defined in (4), the serial transmission of our i th transmitted block $\mathbf{u}_m(i) = \mathbf{C}_m \mathbf{s}_m(i)$ is depicted in Fig. 2 (upper part). Notice that this novel transmission of K symbols over $M(K+L)$ chip periods uses the same block $\mathbf{s}_m(i)$ to “spread each chip” of the code. In contrast, in a conventional direct-sequence (DS) CDMA transmission of K symbols (see the lower part of Fig. 2), each symbol is spread by a short code of length M over a total of MK chip periods.

The received samples $x(n)$ are serial to parallel converted to form $P \times 1$ vectors: $\mathbf{x}(i) := [x(iP), x(iP+1), \dots, x(iP+P-1)]^T$. Define the corresponding noise vector $\boldsymbol{\eta}(i) := [\eta(iP), \eta(iP+1), \dots, \eta(iP+P-1)]^T$; let $\mathbf{H}_{m,0}$ be the $P \times P$ lower triangular Toeplitz matrix with first column $[h_m(0), \dots, h_m(L), 0, \dots, 0]^T$, and $\mathbf{H}_{m,1}$ be the $P \times P$ upper triangular Toeplitz matrix with first row $[0, \dots, 0, h_m(L), \dots, h_m(1)]$. The channel input–output block relationship of our system can be described in matrix-vector form as [27]

$$\mathbf{x}(i) = \sum_{m=0}^{M-1} [\mathbf{H}_{m,0} \mathbf{C}_m \mathbf{s}_m(i) + \mathbf{H}_{m,1} \mathbf{C}_m \mathbf{s}_m(i-1)] + \boldsymbol{\eta}(i) \quad (7)$$

where the second term in the sum accounts for the so-called inter block interference (IBI). On the other hand, our proposed block-spread transmission can be viewed as a symbol-spread transmission (each symbol is spread by the short signature code \mathbf{c}_m) followed by a chip interleaver with guards as shown in Fig. 3. DS-CDMA corresponds to transmitting the interleaver entries row-wise, while our proposed transmitter outputs the interleaver entries column-wise. This not only explains the acronym chip-interleaved block-spread CDMA (CIBS-CDMA), but also highlights how readily implementable (and backward-compatible) the proposed system is by simply cascading to an existing DS-CDMA system a chip interleaver

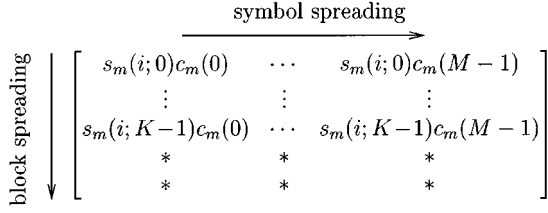


Fig. 3. Redundant chip interleaver.

with guards. Notice that, when $K = 1$ and $L = 0$, it simply reverts to a conventional DS-CDMA system. A chip interleaved transmission has also been advocated in [7]. However, the choice in [7] does not lead to the low-complexity MUI-free reception and symbol detection guarantees that this paper will turn out to possess regardless of multipath. Instrumental to these important multipath-transparent properties are the guard times of length L (see the top of Fig. 2). They introduce redundancy that can be made arbitrarily negligible if one increases the block size K .

Because the last L rows of the matrix \mathbf{C}_m are zero, the IBI is eliminated since $\mathbf{H}_{m,1}\mathbf{C}_m = \mathbf{0}_{P \times K}$. Following (7), the equivalent block-spreading matrix after multipath propagation becomes $\mathbf{H}_{m,0}\mathbf{C}_m$ for the symbol block $\mathbf{s}_m(i)$. Even though \mathbf{C}_m is designed at the transmitter to be orthogonal among users, the convolutive channel will generally destroy this orthogonality and give rise MUI. We next show that the design in (4) preserves the code orthogonality among users even after *unknown* multipath propagation. Multiuser signals can then be separated deterministically using the receive matrix \mathbf{G}_m in (4), which depends only on the desired user's signature code.

Let $\bar{\mathbf{H}}_{m,0}$ be the $(K+L) \times (K+L)$ lower triangular Toeplitz matrix with first column $[h_m(0), \dots, h_m(L), 0, \dots, 0]^T$, $\bar{\mathbf{H}}_{m,1}$ the $(K+L) \times (K+L)$ upper triangular Toeplitz matrix with first row $[0, \dots, 0, h_m(L), \dots, h_m(1)]$, and \mathbf{J}_M an $M \times M$ shift matrix which is defined as the lower triangular Toeplitz matrix with first column $[0, 1, 0, \dots, 0]^T$. We can then split the $P \times P$ matrix $\mathbf{H}_{m,0}$ into smaller blocks and rewrite it as

$$\mathbf{H}_{m,0} = \mathbf{I}_M \otimes \bar{\mathbf{H}}_{m,0} + \mathbf{J}_M \otimes \bar{\mathbf{H}}_{m,1}. \quad (8)$$

Applying (6) and using the fact that $\bar{\mathbf{H}}_{m,1}\mathbf{T}_{zp} = \mathbf{0}_{(K+L) \times K}$, we obtain

$$\begin{aligned} \mathbf{H}_{m,0}\mathbf{C}_m &= \mathbf{c}_m \otimes (\bar{\mathbf{H}}_{m,0}\mathbf{T}_{zp}) \\ &= (\mathbf{c}_m \otimes \mathbf{I}_{K+L})(\mathbf{1} \otimes \bar{\mathbf{H}}_{m,0}\mathbf{T}_{zp}) \\ &= \mathbf{G}_m\bar{\mathbf{H}}_{m,0}\mathbf{T}_{zp}. \end{aligned} \quad (9)$$

We infer from (9) that the code orthogonality among users is preserved since $\mathbf{H}_{m,0}\mathbf{C}_m$ lies in the range space of \mathbf{G}_m and is thus orthogonal to \mathbf{G}_μ for any $\mu \neq m$. In other words, we have

$$\mathbf{G}_\mu^H \mathbf{H}_{m,0}\mathbf{C}_m = \delta(\mu - m)\bar{\mathbf{H}}_{m,0}\mathbf{T}_{zp}. \quad (10)$$

Therefore, using (7) and (10), we can express (2) as

$$\mathbf{y}_\mu(i) = \mathbf{G}_\mu^H \mathbf{x}(i) = \bar{\mathbf{H}}_{\mu,0}\mathbf{T}_{zp}\mathbf{s}_\mu(i) + \mathbf{G}_\mu^H \boldsymbol{\eta}(i). \quad (11)$$

Equation (11) shows how the superposition of received signals from multiple users can be separated deterministically regardless of the unknown FIR multipath channels.

To better understand how the code orthogonality is preserved at the receiver even after frequency-selective filtering, let us divide $\mathbf{x}(i)$ (and similarly $\boldsymbol{\eta}(i)$) into M subblocks of size $(K+L) \times 1$: $\mathbf{x}(i) := [\bar{\mathbf{x}}_0^T(i), \dots, \bar{\mathbf{x}}_{M-1}^T(i)]^T$. For each $n \in [0, M-1]$, we can then express the subblock $\bar{\mathbf{x}}_n(i)$ as [cf. (7) and (4)]

$$\begin{aligned} \bar{\mathbf{x}}_n(i) &= \sum_{m=0}^{M-1} [\bar{\mathbf{H}}_{m,0}\mathbf{T}_{zp}\mathbf{s}_m(i)c_m(n) \\ &\quad + \bar{\mathbf{H}}_{m,1}\mathbf{T}_{zp}\mathbf{s}_m(i)c_m(n-1)] + \bar{\boldsymbol{\eta}}_n(i) \\ &= \sum_{m=0}^{M-1} \bar{\mathbf{H}}_{m,0}\mathbf{T}_{zp}\mathbf{s}_m(i)c_m(n) + \bar{\boldsymbol{\eta}}_n(i) \end{aligned} \quad (12)$$

where, thanks to ZP, inter sub-block interference is avoided. Thus, the n th subblock $\bar{\mathbf{x}}_n(i)$ depends only on the n th chip of each user's spreading code $c_m(n)$, while the adjacent chips from each spreading code do not interfere with each other. Based on (12), the received block $\mathbf{x}(i)$ in (7) can be written as

$$\mathbf{x}(i) = \sum_{m=0}^{M-1} \mathbf{c}_m \otimes (\bar{\mathbf{H}}_{m,0}\mathbf{T}_{zp}\mathbf{s}_m(i)) + \boldsymbol{\eta}(i). \quad (13)$$

As a result, multipath channels with CIBS transmissions cause inter symbol interference (ISI) within each symbol block, which is denoted by $\bar{\mathbf{H}}_{m,0}\mathbf{T}_{zp}\mathbf{s}_m(i)$ in (13), but they *do not give rise to ICI* within the code vector \mathbf{c}_m , i.e., we have replaced ICI by ISI, which maintains the orthogonality among spreading codes at the receiver even after frequency-selective propagation, and enables multiuser separation as confirmed by (11). Replacing ICI by ISI also corroborates our previous discussion [following (4)] that the roles of $\mathbf{s}_m(i)$ and \mathbf{c}_m are interchanged when one compares symbol spreading (bottom of Fig. 2) with block spreading (top of Fig. 2).

Multiplying \mathbf{G}_μ^H with $\mathbf{x}(i)$ amounts to passing $\mathbf{x}(i)$ through a de-interleaver (that is common to all users) and processing the output with a single-user de-spreading filter matched to \mathbf{c}_μ in order to obtain the symbols of each mobile unit (here μ) with ISI corresponding to its own channel. The transceiver for each user is demonstrated in Fig. 4, which consists of symbol spreading (by the short signature code \mathbf{c}_μ) and interleaving at the transmitter, together with de-interleaving and matched filtering (matched to \mathbf{c}_μ) at the receiver. Notice that the code-matching user-separating front-end \mathbf{G}_μ , that provides sufficient statistics for user μ , is para-unitary. Collecting \mathbf{G}_μ 's to form $\mathbf{G} := [\mathbf{G}_1, \dots, \mathbf{G}_M]$, we obtain a $P \times P$ unitary matrix: $\mathbf{G}^H \mathbf{G} = \mathbf{I}_P$. Therefore, if $\boldsymbol{\eta}(i)$ is white, then $\mathbf{G}^H \boldsymbol{\eta}(i)$ remains white and thus multiuser separation with \mathbf{G}_μ in (11) preserves the maximum likelihood (ML) optimality, i.e.,

$$P(\mathbf{x}(i) | \{\mathbf{s}_m(i)\}_{m=0}^{M-1}) = \prod_{m=0}^{M-1} P(\mathbf{y}_m(i) | \mathbf{s}_m(i)) \quad (14)$$

where $P(\cdot | \cdot)$ denotes conditional probability. Therefore, relying on (de-)interleaving and matched filtering operations only [cf. Fig. 4], we have successfully converted a multiuser detection problem, that has to deal with both MUI and ISI due to time-dispersive channels, into a set of equivalent single-user equalization problems without loss of optimality.

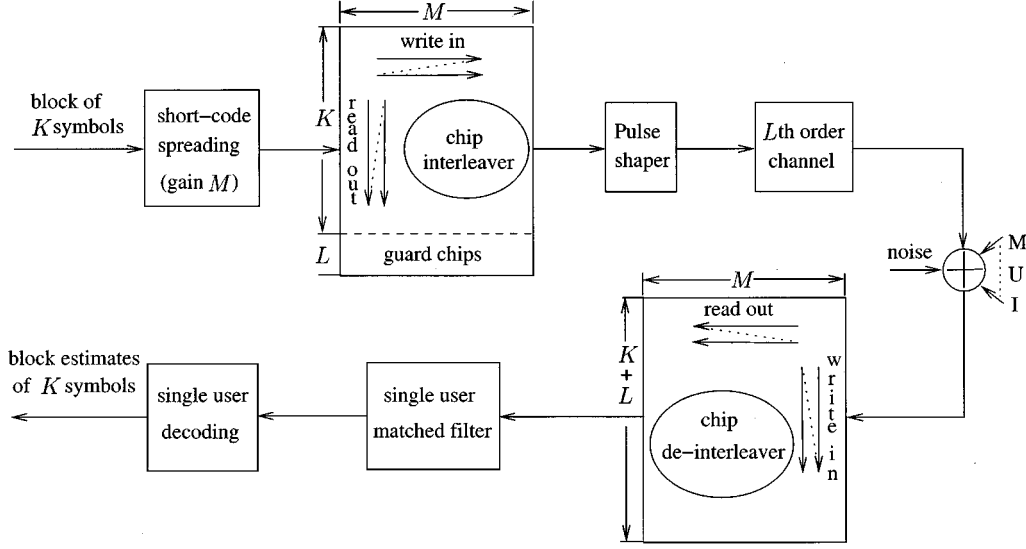


Fig. 4. CIBS-CDMA transceiver for a single user.

After MUI elimination, *any* single-user equalizer can be applied to $\mathbf{y}_\mu(i)$ of (11) to remove the residual ISI. Since the tall Toeplitz matrix $\tilde{\mathbf{H}}_{\mu,0} \mathbf{T}_{\text{zp}}$ of size $(K+L) \times K$ has *always full rank* regardless of the channel zero locations, the symbol block $\mathbf{s}_\mu(i)$ is guaranteed to be detectable in the absence of noise, which is not the case in conventional DS-CDMA systems since signals from different users may cancel each other for some channels [10]. Trading off performance with complexity, we next discuss possible equalization options.

First, notice that $\tilde{\mathbf{H}}_{\mu,0} \mathbf{T}_{\text{zp}} \mathbf{s}_\mu(i)$ expresses nothing but a linear convolution between the symbol vector $\mathbf{s}_\mu(i)$ and the channel vector $\mathbf{h}_\mu := [h_\mu(0), \dots, h_\mu(L)]^T$; hence, the maximum likelihood sequence estimation (MLSE) proposed in [9] is directly applicable. Since \mathbf{h}_μ includes a delay factor that accounts for asynchronism between users, it has at most $\tilde{L}_\mu := \lceil \tau_{\mu,s}/T_c \rceil$ nonzero taps coming from multipath propagation, where $\tau_{\mu,s}$ denotes the multipath spread of the μ th user's channel. For constellations of size Q , the complexity of MLSE, using Viterbi's algorithm, reduces to $O(KQ^{\tilde{L}_\mu})$ per symbol block or $O(Q^{\tilde{L}_\mu})$ per symbol. Thus, the decoding complexity per symbol only depends on the constellation size Q and the effective channel order \tilde{L}_μ , and is irrespective of the block length K and the maximum channel order L . Therefore, optimal MLSE demodulation becomes feasible for channels with small multipath spread; the value of \tilde{L}_μ is obtained at the receiver following channel estimation.

When \tilde{L}_μ is large preventing the usage of MLSE, we resort to linear equalization for moderate block size K . Defining $\check{\mathbf{H}}_\mu := \tilde{\mathbf{H}}_{\mu,0} \mathbf{T}_{\text{zp}}$ for notational brevity, we can adopt the linear ZF equalizer given by

$$\mathbf{I}_\mu^{\text{zf}} = [\check{\mathbf{H}}_\mu^H \check{\mathbf{H}}_\mu]^{-1} \check{\mathbf{H}}_\mu^H \quad (15)$$

to eliminate ISI at the price of noise enhancement. Taking into account the noise explicitly, the linear MMSE equalizer can be also used. In block (matrix) form, it is expressed as

$$\mathbf{I}_\mu^{\text{mmse}} = [\check{\mathbf{H}}_\mu^H \check{\mathbf{H}}_\mu + (\sigma_\eta^2/\sigma_s^2) \mathbf{I}_K]^{-1} \check{\mathbf{H}}_\mu^H \quad (16)$$

where we have assumed that $E\{\mathbf{s}_\mu(i) \mathbf{s}_\mu^H(i)\} = \sigma_s^2 \mathbf{I}_K$ and $E\{\boldsymbol{\eta}(i) \boldsymbol{\eta}^H(i)\} = \sigma_\eta^2 \mathbf{I}_P$ (extension to colored noise is straight-

forward). Inverting a general $K \times K$ matrix incurs complexity $O(K^3)$. However, by exploiting the fact that $\check{\mathbf{H}}_\mu^H \check{\mathbf{H}}_\mu$ in (15) and $\check{\mathbf{H}}_\mu^H \check{\mathbf{H}}_\mu + (\sigma_\eta^2/\sigma_s^2) \mathbf{I}_K$ in (16) are Hermitian positive definite Toeplitz matrices, the complexity required for their computation and inversion is reduced to $O(K^2)$ [13, p. 197]. Therefore, the overall linear equalization by (15) or (16) incurs complexity $O(K^2)$.

When the channel order L and thus the block size K increase to render even the linear equalizers of (15) and (16) complex, we recommend using a low-complexity frequency domain equalization which takes advantage of the Toeplitz structure of $\tilde{\mathbf{H}}_{\mu,0} \mathbf{T}_{\text{zp}}$, as we detail next (see also [23], [8], and [19]).

Let \mathbf{I}_{zp} denote the first L columns of \mathbf{I}_K and define the $K \times (K+L)$ matrix $\mathbf{R}_{\text{zp}} := [\mathbf{I}_K, \mathbf{I}_{\text{zp}}]$. Notice that post-multiplying \mathbf{R}_{zp} by a $(K+L) \times 1$ vector maps it to a $K \times 1$ vector by overlapping-and-adding the last L elements to its first L elements (matrix implementation of the overlap-add operation in block convolution). Thus, we can always convert the Toeplitz matrix $\tilde{\mathbf{H}}_{\mu,0} \mathbf{T}_{\text{zp}}$ into a circulant one through \mathbf{R}_{zp} as follows: $\check{\mathbf{H}}_\mu := \mathbf{R}_{\text{zp}} \tilde{\mathbf{H}}_{\mu,0} \mathbf{T}_{\text{zp}}$. Because (IFFT)'s diagonalize circulant matrices, the circulant matrix $\check{\mathbf{H}}_\mu$ can be decomposed (see [27] for details) as $\check{\mathbf{H}}_\mu = \mathbf{F}_K^H \mathbf{D}_{h,\mu} \mathbf{F}_K$, where $\mathbf{D}_{h,\mu}$ is a diagonal matrix with $(k+1)$ st diagonal entry: $H_\mu(e^{-j2\pi k/K}) := \sum_{l=0}^L h_\mu(l) e^{-j2\pi kl/K}$. Therefore, we can design our low-complexity (LC) equalizer³ for user μ as

$$\mathbf{I}_\mu^{\text{lc}} = \mathbf{F}_K^H [\mathbf{D}_{h,\mu}^H \mathbf{D}_{h,\mu} + (\sigma_\eta^2/\sigma_s^2) \mathbf{I}_K]^{-1} \mathbf{D}_{h,\mu}^H \mathbf{F}_K \mathbf{R}_{\text{zp}}. \quad (17)$$

Matrix $\mathbf{I}_\mu^{\text{lc}}$ equalizes the channel in the frequency domain and its complexity no longer depends on the channel order L as opposed to conventional time-domain equalizers [8]. Since $\mathbf{I}_\mu^{\text{lc}}$ in (17) includes only two fast Fourier transform (FFT) operations and a diagonal matrix inversion, it has low complexity of order $O(2K \log_2 K)$ per symbol block. However, symbol detection is

³Notice that the noise is slightly colored by the matrix \mathbf{R}_{zp} before FFT processing, but the noise color becomes negligible as K increases and can be omitted when $K \gg L$. Alternatively, we can pursue frequency domain equalization without coloring the noise by taking an FFT of size $K+L$ directly [19].

not guaranteed since there exist channels $H_\mu(z)$ that have nulls located at $z = e^{-j2\pi k/K}$, such that $\mathbf{D}_{h,\mu}$ (and hence $\tilde{\mathbf{H}}_\mu$) loses rank and becomes noninvertible.

Two important remarks are now in order.

Remark 1 (ISI Versus MUI): CIBS-CDMA replaces ICI by ISI, and thereby converts a multiuser detection problem into a set of equivalent single-user equalization problems. It is thus of interest to compare it with conventional multiuser detection-based approaches.

A) Performance and Complexity: The performance and complexity depend on the specific choice of the equalizer and the multiuser detector, which in turn are related to the operating system parameters. While general comparisons on these issues are difficult without detailed system specifications, we refer the reader to a particular comparison example carried out in [16] between the MUI-free transceiver of [16] and the linear multiuser detector of [17], both utilizing blind subspace-based channel estimation and ZF equalization.

B) Flexibility and Robustness: Notice that equalization among users in CIBS-CDMA is fully uncoordinated, and each user may choose an equalizer depending on her/his own computational capability, without interfering with other users. This is in sharp contrast with joint (and thus fully coordinated) multiuser detectors. The fundamental distinction originates from the different multiple access philosophies: conventional DS-CDMA schemes allow for fully uncoordinated transmissions but pay off in coordinated joint multiuser detection; while MUI-free transceivers, including the proposed one and those in [22], [11], and [15], rely on minimally coordinated transmissions to achieve uncoordinated detection. We believe that this uncoordinated detection capability favors MUI-free transceivers because it enhances their robustness to imperfect system parameters, e.g., imperfect channel estimates and unbalanced power control [29]; intuitively speaking, poor channel estimation accuracy from one user does not affect other users' performance. However, thorough investigation of these issues goes beyond the scope of this paper.

Remark 2 (Delay Control Versus Power Control): As mobile users are distributed, the power received from each user may have a large dynamic range, which necessitates stringent power control for multiuser detection. However, power control requirements are alleviated in CIBS-CDMA since the received signals from multiple users are separable by design. The key parameter, however, in the CIBS-CDMA is the maximum channel order L . Large L implies large K to achieve high bandwidth efficiency (see discussions later on in Section III-A), which increases decoding complexity and decoding delay.⁴ It is thus favorable to keep L as small as possible. As we have discussed earlier, $L = \lceil (\tau_{\max,s} + \tau_{\max,a})/T_c \rceil$ depends on $\tau_{\max,a}$ and $\tau_{\max,s}$. Notice that $\tau_{\max,s}$ is determined by the operating environment and is thus not up to the designer's control. To maintain a small channel order L , we may rely on delay control to decrease $\tau_{\max,a}$. In this case, each mobile user synchronizes with the base station's pilot waveform and roughly calculates the distance from the base station by, e.g., power measurements. In the

⁴The decoding delay induced by K might not be a problem, since in practical systems error control coding is used with an interleaver, which typically introduces an even larger delay.

reverse link, the mobile advances its transmissions by a corresponding amount to compensate for the two-way propagation time that is consumed between the base station and the mobile user. With such a delay control mechanism, the maximum $\tau_{\max,a}$ could be considerably reduced.

We next compare the proposed transceiver design with those in [11], [27], [15], and [16] that also achieve deterministic MUI elimination and guarantee symbol detectability; actually, they arrive at the same output (cf. (11) with [11, eq. (19)] and [16, eq. (9)]). Our first metric for comparison will be bandwidth efficiency.

A. Bandwidth Efficiency

Within each received $P \times 1$ block $\mathbf{x}(i)$ in (7), K information symbols are transmitted per user. The bandwidth efficiency for M users can thus be calculated as

$$\mathcal{E}_1 = \frac{MK}{M(K+L)} = \frac{K}{K+L}. \quad (18)$$

Note that the bandwidth efficiency for the AMOUR system in [11] is: $\mathcal{E}'_1 = MK/[M(K+L)+L]$. When $L \ll M(K+L)$, we obtain $\mathcal{E}_1 \approx \mathcal{E}'_1$. On the other hand, choosing $K \gg L$ enables \mathcal{E}_1 and \mathcal{E}'_1 to approach 1, which indicates that both systems have high bandwidth efficiency⁵. In contrast, the codes in [15], [16] are designed to be shift orthogonal, which constrains their length to equal twice the number of users plus one. Thus, with our notation, the bandwidth efficiency in [15] and [16] is

$$\mathcal{E}_2 = \frac{MK}{2MK+K} = \frac{M}{2M+1} < 50\%. \quad (19)$$

Selecting the information block size $K \geq L$ as in [15] and [16], we find from (18) and (19) that

$$\mathcal{E}_1 \approx \mathcal{E}'_1 \geq 50\% > \mathcal{E}_2. \quad (20)$$

Another way to look at bandwidth efficiency is to calculate the maximum number of users (with guaranteed MUI elimination and symbol detectability) that can be accommodated by the available system bandwidth. Suppose the system is allocated bandwidth W and the information rate is R_b . The spreading gain is thus $N = W/R_b$. For AWGN channels, the maximum number of users that do not interfere with each other is N when employing either TDMA, FDMA, or CDMA. In our system (and [11]), the spreading gain is $P/K = M(K+L)/K$ and thus, the maximum number of MUI-free users is

$$M = \frac{K}{K+L}N \quad (21)$$

while in [15] and [16] the maximum number is $(N-1)/2$, and $N-1$ is restricted to be a power of 2.

To illustrate the difference between our system and [15] and [16], we compare in Fig. 5 the corresponding bandwidth efficiencies for channels of maximum order $L = 1$ (2-rays) and $L = 3$ (4-rays) with K varying from 1 to 16. Setting the

⁵Notice that the block duration PT_c should be sufficiently smaller than the channel coherence time, so that the channels we consider are time-invariant within each block. Therefore, the present version of our system is not applicable to fast fading channels. For slowly fading channels, the coherence time might also limit the maximum value of K , which in turn determines the highest possible bandwidth efficiency.

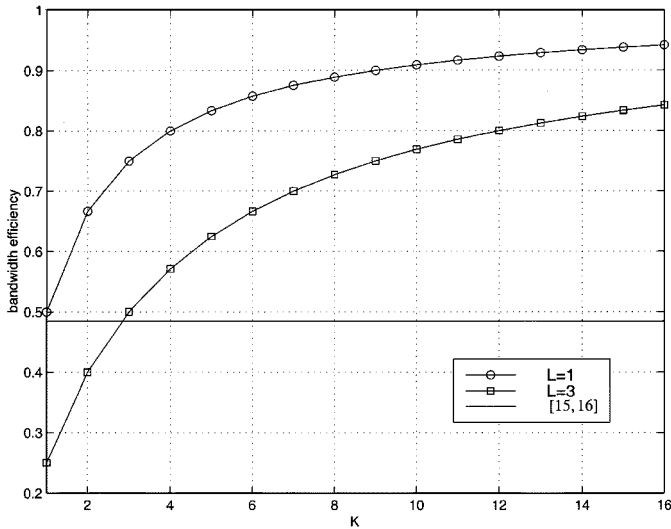


Fig. 5. Bandwidth efficiency.

spreading gain to $N = 33$, Fig. 6 shows the maximum number of MUI-free users that are allowed. Certainly, with increasing K , our system can accommodate many more users than can [15] and [16].

B. Complexity and Design Flexibility

In this subsection, we will compare the computational complexity among the three different MUI-resilient transceivers: this paper's and those in [11], [27], [15], [16]. First, we note that all three transceivers arrive at the same single user block model (11); hence, the complexity of blind channel estimators and equalizers is identical. The main difference lies in the multiuser separating front-end matrices \mathbf{G}_m . For this reason, we only concentrate on the complexity differences among the three front-ends.

For each user in CIBS-CDMA, the front-end amounts to $K + L$ inner products between $M \times 1$ vectors. Since each correlator of length M requires M multiplies and $M - 1$ adds, its complexity is $O(M)$. So the complexity per user is $O(M(K + L))$, and the overall complexity for all users (e.g., at the base station (BS) where we need to demodulate all users' information) is $O(M^2(K + L))$. With M users in [15] and [16], the shift-orthogonal codes have length $2M + 1$, and consequently each receiver needs $K + L$ inner products between $2M \times 1$ vectors after discarding 1 cyclic prefix. Therefore, each user in [15] and [16] has complexity of order $O(2M(K + L))$, and the overall complexity for M users will be $O(2M^2(K + L))$.

Unlike [15] and [16], where only a special class of codes with 50% bandwidth efficiency is constructed, and different from [11], where highly efficient codes are generally complex, the design herein is very flexible because the only requirement on our spreading codes is their mutual orthogonality. Since the design of orthogonal codes has been well developed in the literature (at least for multipath-free propagation), there are many fast algorithms available. Using such algorithms, the complexity of our transceivers can be lowered even further. For example, we can adopt inverse FFT (IFFT) or Walsh-Hadamard (W-H) codes for the code-generating vector \mathbf{c}_m in (4). Then, at the BS,

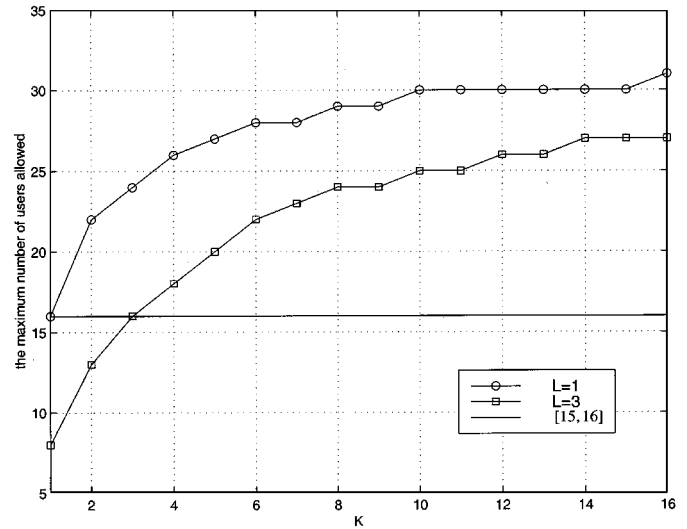


Fig. 6. The maximum number of users allowed.

we can apply FFT or Fast Walsh Transform (FWT) to separate users. If the FFT is employed, the complexity for all users is $O(M(\log_2 M)(K + L))$, while the FWT is even faster than the FFT [2]. Recall though that W-H codes with length N exist only if $N/4$ is an integer [12]. But, even if we constrain our codes to be W-H, the requirement on the code length N of [15] and [16] is more restrictive since $N - 1$ is required to be a power of 2.

For each user in [11], the front-end consists of $K + L$ inner products between the $P \times 1$ received block and different Vandermonde vectors. So, the complexity per user is $O(P(K + L))$, while the overall complexity for M users will be $O(MP(K + L))$. Note that AMOUR codes can also be constructed based on FFTs to reduce computational complexity. If \mathbf{G}_m are columns of the $P \times P$ FFT matrix, the front-end for all users amounts to a P -point FFT and AMOUR's complexity reduces to $O(P(\log_2 P)(K + L))$. The simplest AMOUR code was proposed in [27, eq. (25)] and can be expressed as

$$\mathbf{C}_m = \mathbf{f}_m \otimes \mathbf{T}_{zp} \quad (22)$$

where \mathbf{f}_m is the m th column of the $M \times M$ FFT matrix. Since the code set $\{\mathbf{f}_m\}_{m=0}^{M-1}$ satisfies d1), it is subsumed in our code designs herein; hence, the resulting receiver has complexity $O(M(\log_2 M)(K + L))$.

For clarity, we summarize complexity requirements and comparisons with [11], [27], [15], and [16] in Table I. If the system has more than $\log_2 M$ active users, it is better to use fast algorithms rather than separate correlators at the BS. With the same number of users, we infer from Table I that our system has less complexity than [15] and [16], and the difference becomes more pronounced if special codes (e.g., W-H or FFT) are employed. Fast algorithms for the codes in [15], [16] have not been reported.

Another remark here is that if we apply the equalizer (17), which requires only two FFTs, low-complexity MUI and ISI elimination per user becomes possible provided that the channel can also be obtained with low-complexity methods (e.g., via training, or, with the finite-alphabet based algorithm outlined in

TABLE I
COMPLEXITY OF MULTIUSER SEPARATING FRONT-END

	single user	M users	FFT (or FWT) based algorithms
this paper	$O(M(K+L))$	$O(M^2(K+L))$	$O(M(\log_2 M)(K+L))$
[15, 16]	$O(2M(K+L))$	$O(2M^2(K+L))$	not available
[11, 27]	$O(P(K+L))$	$O(MP(K+L))$	$O(M(\log_2 M)(K+L))$

Section V-B). If channel estimation is complex or if the channel is varying fast and CSI needs to be updated frequently, the complexity of the multiuser separating front-end is less critical for the overall receiver design.

C. Perfectly Constant Modulus Uplink Transmissions

A well-known drawback of multicarrier systems is that the transmitted signal is not of constant modulus, which imposes restrictions on the system hardware design and undesirable back-offs in the high-power amplifier (HPA). Note that the uplink transmissions in [15] have constant modulus, while our system and the FFT-based designs of [11] and [27] have constant modulus except for the guard zeros. Although not a problem for the HPA, usage of guard zeros may cause on/off implementation problems in analog system designs. However, with a digital signal processing (DSP) unit and a digital-to-analog converter (D/A) at the transmitter, inserting zeros is not a problem for, e.g., software radio systems [20]. Nevertheless, as we detail next, the proposed transmitter can also dispense with zero padding and achieve perfectly constant modulus transmissions during its uplink operation.

With the code design in (4), the $P \times 1$ transmitted block $\mathbf{u}_m(i) = \mathbf{C}_m \mathbf{s}_m(i)$ has M zero subblocks of length L evenly distributed across each block. To make up for perfectly constant modulus, we fill in the zero gaps using $L \times 1$ nonzero vectors with entries drawn from the same constellation as $\mathbf{s}_m(i)$, that is, we modify the transmitter as

$$\check{\mathbf{u}}_m(i) = \mathbf{C}_m \mathbf{s}_m(i) + \check{\mathbf{b}}_m, \quad \check{\mathbf{b}}_m := \mathbf{1}_{M \times 1} \otimes [\mathbf{0}_{K \times 1}^T, \mathbf{b}_m^T]^T. \quad (23)$$

In this case, the modified transmitted block $\check{\mathbf{u}}_m(i)$ has perfectly constant modulus across the block. We next show that these filling vectors do not change our receiver design provided that the codes are selected to have zero mean.

With the modified block $\check{\mathbf{u}}_m(i)$ in (23), and the original received vector $\mathbf{x}(i)$ in (7), the new received vector $\check{\mathbf{x}}(i)$ can be expressed as

$$\check{\mathbf{x}}(i) = \mathbf{x}(i) + \sum_{m=0}^{M-1} (\mathbf{H}_{m,0} \check{\mathbf{b}}_m + \mathbf{H}_{m,1} \check{\mathbf{b}}_m). \quad (24)$$

Thus, our task is to show that $\mathbf{G}_\mu^H \check{\mathbf{x}}(i) = \mathbf{G}_\mu^H \mathbf{x}(i)$, which is equivalent to verifying that

$$\mathbf{G}_\mu^H (\mathbf{H}_{m,0} + \mathbf{H}_{m,1}) \check{\mathbf{b}}_m = \mathbf{0}, \quad \forall m, \mu \in [0, M-1]. \quad (25)$$

Note that $\mathbf{H}_{m,1}$ can be expressed as $\mathbf{J}_M^{-(M-1)} \otimes \bar{\mathbf{H}}_{m,1}$, where $\mathbf{J}_M^{-(M-1)}$ denotes the $-(M-1)$ st power of \mathbf{J}_M , which has only one unit entry at the top-right corner, and zeros elsewhere.

Introducing the matrix $\mathbf{Z}_M := \mathbf{J}_M + \mathbf{J}_M^{-(M-1)}$ that performs a cyclic shift on a vector, and using the block-expression of $\mathbf{H}_{m,0}$ in (8), we then obtain

$$\mathbf{H}_{m,0} + \mathbf{H}_{m,1} = \mathbf{I}_M \otimes \bar{\mathbf{H}}_{m,0} + \mathbf{Z}_M \otimes \bar{\mathbf{H}}_{m,1}. \quad (26)$$

With the receive matrix \mathbf{G}_μ designed as in (4) and with $\check{\mathbf{b}}_m$ inserted from (23), we arrive at

$$\begin{aligned} \mathbf{G}_\mu^H (\mathbf{H}_{m,0} + \mathbf{H}_{m,1}) \check{\mathbf{b}}_m &= (\mathbf{c}_\mu^H \mathbf{1}_{M \times 1}) \otimes \left(\bar{\mathbf{H}}_{m,0} [\mathbf{0}_{K \times 1}^T, \mathbf{b}_m^T]^T \right) \\ &\quad + (\mathbf{c}_\mu^H \mathbf{Z}_M \mathbf{1}_{M \times 1}) \otimes \left(\bar{\mathbf{H}}_{m,1} [\mathbf{0}_{K \times 1}^T, \mathbf{b}_m^T]^T \right) \\ &= (\mathbf{c}_\mu^H \mathbf{1}_{M \times 1}) \otimes (\bar{\mathbf{H}}_{m,0} + \bar{\mathbf{H}}_{m,1}) [\mathbf{0}_{K \times 1}^T, \mathbf{b}_m^T]^T \end{aligned} \quad (27)$$

where the identity $\mathbf{Z}_M \mathbf{1}_{M \times 1} = \mathbf{1}_{M \times 1}$ was used in establishing the second equality.

Therefore, (27) leads to (25) if in addition to d1) we adopt the design constraint of:

d2) balanced user codes; i.e., $\mathbf{c}_\mu^H \mathbf{1}_{M \times 1} = \mathbf{0}, \forall \mu \in [0, M-1]$.

Note that d2) is not very restrictive and can be satisfied by many code designs. For instance, IFFT or W-H codes satisfy d2) after discarding only the code with all one entries. The maximum number of users is thus only decreased by one. Recall however that with the filling symbols in (23), we achieve a perfectly constant modulus transmission while maintaining its low-complexity MUI/ISI-resilient reception and its high bandwidth efficiency regardless of frequency-selective multipath.

The penalty with nonzero guards is a small power loss since we allocate $ML/MK = L/K$ percent of the transmit-power to the filling symbols. However, if $K \gg L$, the power loss is small. Furthermore, the power loss can be reduced further since the transmitters do not need to pick the same amplitude for the filling symbols as for the data symbols. If the amplitude of the filling symbols is reduced by half, the power loss decreases to one fourth of the original one. The extreme case is to insert filling symbols with zero amplitude as in (4), which incurs no power loss. Note that the filling symbols can be designed to have arbitrary shape to facilitate analog hardware implementation. Furthermore, being known to the receiver, the filling symbols can also be utilized for possible synchronization, or channel estimation purposes, e.g., by following the approaches in [6]. However, these topics go beyond the scope of this paper and will not be discussed here. In the next section, we will introduce variants of the proposed transceiver, which do not insert zeros at the transmitter.

IV. EXTENSIONS

Motivated by the possibility of using either CP or ZP in single-user OFDM systems [27], [19], we can also employ CP-based multiuser transmissions to obtain block-spread transmissions with perfectly constant modulus.

A. Cyclic Prefixed Transmissions

Let \mathbf{I}_{cp} denote the matrix formed by the last L rows of \mathbf{I}_K and define the $(K+L) \times K$ transmit-matrix $\mathbf{T}_{cp} := [\mathbf{I}_{cp}^T, \mathbf{I}_K]^T$ that inserts the CP, and the $K \times (K+L)$ receive-matrix $\mathbf{R}_{cp} =$

$[\mathbf{0}_{K \times L}, \mathbf{I}_K]$ that discards the CP. We can then replace the ZP transceiver in (4) by

$$\mathbf{C}_m = \mathbf{c}_m \otimes \mathbf{T}_{\text{cp}}, \quad \mathbf{G}_m = \mathbf{c}_m \otimes \mathbf{R}_{\text{cp}}^T. \quad (28)$$

Because the first L columns of \mathbf{G}_m are zero, the IBI is removed since $\mathbf{G}_\mu^H \mathbf{H}_{m,1} = \mathbf{0}, \forall \mu \in [0, M-1]$. Similar to (10) and with $\mathbf{R}_{\text{cp}} \bar{\mathbf{H}}_{m,1} = \mathbf{0}$, we can readily verify by direct substitution that

$$\mathbf{G}_\mu^H \mathbf{H}_{m,0} \mathbf{C}_m = \delta(m-\mu) \mathbf{R}_{\text{cp}} \bar{\mathbf{H}}_{m,0} \mathbf{T}_{\text{cp}}. \quad (29)$$

The output of our multiuser separating front-end then becomes

$$\mathbf{G}_\mu^H \mathbf{x}(i) = \mathbf{R}_{\text{cp}} \bar{\mathbf{H}}_{\mu,0} \mathbf{T}_{\text{cp}} \mathbf{s}_\mu(i) + \mathbf{G}_\mu^H \boldsymbol{\eta}(i). \quad (30)$$

Equation (30) shows that $\mathbf{G}_\mu^H \mathbf{x}(i)$ is MUI-free, which enables application of any single-user equalizer. Because the equivalent channel matrix $\bar{\mathbf{H}}_\mu := \mathbf{R}_{\text{cp}} \bar{\mathbf{H}}_{\mu,0} \mathbf{T}_{\text{cp}} = \mathbf{F}_K^H \mathbf{D}_{h,\mu} \mathbf{F}_K$ is circulant, each single-user receiver can employ the low-complexity matrix equalizer as in (17)

$$\mathbf{\Gamma}_\mu^{\text{cp}} = \mathbf{F}_K^H [\mathbf{D}_{h,\mu}^H \mathbf{D}_{h,\mu} + (\sigma_\eta^2 / \sigma_s^2) \mathbf{I}_K]^{-1} \mathbf{D}_{h,\mu}^H \mathbf{F}_K. \quad (31)$$

The advantage of CP over ZP is that the CP transmitter achieves perfect constant modulus in the uplink. However, the price paid is possible performance loss⁶ because the circulant matrix $\bar{\mathbf{H}}_\mu$ could lose rank if the channel $H_\mu(z)$ has nulls located at $z = e^{j2\pi k/K}$ for $k \in [0, K-1]$. If $\bar{\mathbf{H}}_\mu$ is noninvertible (or ill-conditioned), the symbols cannot be recovered. Therefore, unlike ZP where the Toeplitz matrix $\bar{\mathbf{H}}_{\mu,0} \mathbf{T}_{\text{cp}}$ is always full rank, detection of user symbols is not guaranteed with CP.

B. Precoding or Error-Control Coding for CP Transmissions

To guarantee symbol detection with our CP transceivers, we can employ redundant precoding or error-control (channel) coding at the expense of some information rate loss. In other words, instead of transmitting the $K \times 1$ data vector $\mathbf{s}_m(i)$, we can transmit a $K' \times 1$ vector $\mathbf{s}'_m(i)$ with $K' > K$. Vector $\mathbf{s}'_m(i)$ could denote a channel encoded sequence (with, e.g., block or convolutional coding), or, a linearly precoded block obtained by premultiplying $\mathbf{s}_m(i)$ with a tall $K' \times K$ matrix $\boldsymbol{\Theta}_m$ with entries from the complex field. For linear precoding, the transmitted i th block is now $\mathbf{s}'_m(i) = \boldsymbol{\Theta}_m \mathbf{s}_m(i)$, and the receiver output in (30) becomes

$$\begin{aligned} \mathbf{G}_\mu^H \mathbf{x}(i) &= \tilde{\mathbf{H}}_\mu \boldsymbol{\Theta}_m \mathbf{s}_m(i) + \mathbf{G}_\mu^H \boldsymbol{\eta}(i) \\ &= \mathbf{F}_{K'}^H \mathbf{D}_{h,\mu} \mathbf{F}_{K'} \boldsymbol{\Theta}_m \mathbf{s}_m(i) + \mathbf{G}_\mu^H \boldsymbol{\eta}(i). \end{aligned} \quad (32)$$

Note that the diagonal matrix $\mathbf{D}_{h,\mu}$ has at most L zeros since all channels have maximum order L . Therefore, if $K' - K \geq L$ and the precoder $\boldsymbol{\Theta}_m$ is chosen so that any K rows of $\mathbf{F}_{K'} \boldsymbol{\Theta}_m$ are linearly independent, then the matrix $\mathbf{D}_{h,\mu} \mathbf{F}_{K'} \boldsymbol{\Theta}_m$ will have full column rank and the detection of $\mathbf{s}_\mu(i)$ will be guaranteed (see also [10], [11], and [27] for a similar argument and choices of $\boldsymbol{\Theta}_m$ precoding matrices). To assure symbol detectability, only a slight loss in bandwidth efficiency is incurred. The latter now

⁶Notice that the ML optimality is lost since the discarded chips also contain useful information.

becomes $MK/[M(K'+L)] < \mathcal{E}_1$. However, bandwidth efficiency can be regained by increasing K and $K' (= K+L)$ at the expense of a slight increase in decoding complexity and decoding delay. Note also that the constant modulus is generally not assured with linear precoding, although we avoid transmitting zeros within blocks.

C. Loading ZP or CP Transmissions

The equalizers (17) for ZP and (31) for CP entail two FFTs at the receiver. As with single-user OFDM systems [4], one FFT operation can be moved to the transmitter, which amounts to linear precoding with the IFFT matrix as follows:

$$\mathbf{s}'_m(i) = \mathbf{F}_K^H \mathbf{s}_m(i) \quad (33)$$

where $\mathbf{s}'_m(i)$ now denotes the $K \times 1$ transmitted block. Then, easy frequency-domain equalization can be accomplished with one FFT and scalar division at the receiver. By using nonredundant IFFT precoding at the transmitter, the frequency-selective channel for each user is further converted to parallel flat-faded subchannels as in single-user OFDM [4]. Therefore, power and bit loading can be applied across subchannels for each user, exactly as with discrete multiple tone (DMT) modulation (see e.g., [21]). That is, we can replace (33) by

$$\mathbf{s}'_m(i) = \mathbf{F}_K^H \boldsymbol{\Lambda}_m \mathbf{s}_m(i) \quad (34)$$

where $\boldsymbol{\Lambda}_m$ is a diagonal matrix with diagonal entries allocating power across the single user subchannels.

More generally, we can precode with no redundancy ($K' = K$) the information block $\mathbf{s}_m(i)$ by any full rank $K \times K$ matrix (let us denote it by $\bar{\mathbf{F}}_K$ here) $\mathbf{F}_K^H \mathbf{s}'_m(i) = \bar{\mathbf{F}}_K \mathbf{s}_m(i)$. Under several criteria, the optimal loading matrices $\bar{\mathbf{F}}_K$ for ZP transceivers were developed in [24]. Therefore, with the low-complexity multiuser separating front-end, we recognize that schemes developed for single-user systems can be applied directly to multiuser scenarios.

The redundant precoding in Section IV-B and the nonredundant loading of this section will again lead to nonconstant modulus transmissions. However, since the precoding and loading are performed over blocks of length K , the peak to average ratio (PAR) depends on the size of K , rather than $P = O(M(K+L))$, which is the case in AMOUR [11]. Since $K \ll P$, the nonlinear effects are thus expected to be less severe here even with precoding or loading.

V. CHANNEL ESTIMATION ISSUES

To demodulate user information, we need to acquire CSI at the receiver that is required by either linear or nonlinear equalizers [cf. (15), (16), or (17)]. Since multiuser transmissions are converted to parallel single-user transmissions, blind or nonblind channel estimation methods developed for single-user transmissions can be applied directly. Next, we summarize briefly the available schemes for the options described in Sections III and IV.

Certainly, training-based CSI acquisition is one candidate. Note that, unlike the traditional multiuser setup, the training sequences for all users do not need to be designed jointly. However, training sequences consume bandwidth especially when

the underlying channel is varying and frequent re-training is required. (Semi-) blind channel estimators attract growing interest for such cases.

A. Subspace-Based Channel Estimation

Based on the data model (11) for ZP transmissions, the subspace-based method of [24] is an option that guarantees channel identifiability regardless of the FIR channel zero locations. Correspondingly, for the CP transceiver in (30), the subspace-based channel estimation developed in [18] can be utilized. In this case, however, each channel is identifiable provided that its roots are not on (or close to) the FFT grid: $e^{j2\pi k/K}$, $k \in [0, K-1]$.

When the CP transceiver is equipped with precoding as in (32), the blind subspace method of [10] is preferable, because it is also proven to guarantee channel identifiability if K' is chosen to satisfy $K' - K \geq L$ with any K rows of $\mathbf{F}_{K'} \Theta_\mu$ designed to be linearly independent.

Because subspace-based methods capitalize only on data structure information, they are appropriate for any signal constellation. They can still be applied to the systems with nonredundant precoding (and loading) that we described in Section IV-C. The drawbacks of subspace-based approaches are: i) they require many data blocks, which assumes that the channel is varying sufficiently slow, and ii) when K is large, their complexity increases since they involve singular value decomposition (SVD). However, if the appropriate precoding matrix is applied, low-complexity channel estimators become possible as we discuss next.

B. (Semi-) Blind Finite-Alphabet-Based Channel Estimation

If the FFT precoder of (33) [or (34)] is applied, we arrive at a single-user OFDM transmission model for each user. All methods that have been developed for single-user OFDM can thus be applied here including the subspace-based approaches of [24] and [18]. Based on the finite alphabet (FA) property of the source symbols, a new low-complexity channel estimator method was proposed recently in [30], which guarantees channel identifiability regardless of channel zeros if one selects $K > 2L$ for BPSK, or $K > 4L$ for QPSK and QAM signals. Furthermore, the FA-based approach can estimate the channel with only one block for PSK constellations, which implies that it can track faster channel variations than the subspace-based approaches. If used together with training sequences at the beginning of the data transmission, the semi-blind adaptive implementation of [30] can track slow channel variations with high accuracy and surprisingly low complexity. Therefore, with FA-based channel estimation, the overall multiuser receiver has very low complexity.

VI. PERFORMANCE ANALYSIS AND SIMULATIONS

Since the signals from multiple users are separated at the receiver, we can analyze the performance for each user separately. If the ZF equalizer in (15) is employed, theoretical BER evaluation becomes possible [11]. For simplicity, we here focus only on BPSK signals. Assuming that the noise $\eta(n)$ in (1) is white with zero mean and variance $N_0/2$, the noise block $\mathbf{G}_\mu^H \boldsymbol{\eta}(i)$ in

(11) has correlation matrix $(N_0/2)\mathbf{I}_{K+L}$ thanks to the orthogonality between the columns of \mathbf{G}_μ . Let us denote the k th column of the ZF equalizer $\boldsymbol{\Gamma}_\mu^{z,f}$ of (15) as $\gamma_{\mu,k}$. With E_b/N_0 standing for the bit SNR, the average BER for user μ is thus (see also [11])

$$\bar{P}_{e,\mu} = \frac{1}{K} \sum_{k=0}^{K-1} \mathcal{Q} \left(\frac{1}{\|\gamma_{\mu,k}\|} \sqrt{\frac{2E_b}{N_0}} \right) \quad (35)$$

where $\|\cdot\|$ is the Euclidean norm of a vector and $\mathcal{Q}(\cdot)$ denotes the \mathcal{Q} -function. Note that the BER in (35) is channel-dependent. In the following test cases, we will look at the average BER over 5 000 Monte Carlo channel realizations where the FIR channels are randomly generated with each tap being Rayleigh distributed.

Test Case 1 (Comparison With Multiuser Detectors): To compare the proposed CIBS transceivers with symbol-spread multiuser detectors, we simulate both direct sequence (DS) CDMA and multi-carrier (MC) CDMA systems. The system spreading gain is $N = 19$ and the channels have maximum order $L = 3$ (4-rays). The DS-CDMA users spread their information symbols with W-H spreading codes of length $N - L = 16$ and insert 3 zeros between blocks to avoid IBI/ISI. The MC-CDMA users adopt OFDM with CP of length 3 after spreading their information symbols with W-H codes of length 16. When only the channel of the desired user is available, the single-user RAKE receiver can be employed. The corresponding BER curve levels off and a high error floor appears due to the MUI, resulting a poor performance far from that of single user case⁷, as shown in Fig. 7. To remove MUI, we also simulated ZF and MMSE⁸ multiuser detectors for both DS-CDMA and MC-CDMA, which require knowledge of the codes and the channels of all users at the receiver-end. For the proposed transceiver, we simulated two scenarios. The first uses $K = 6$ to accommodate $M = 12$ users [cf. (21)]. The second adopts $K = 16$, which enables MUI-free reception of $M = 16$ users. Increasing the block size K allows for more MUI-free users [cf. (21)]; however, the BER performance per user degrades as illustrated in Fig. 7 (it will be further elaborated in Test Case 2). Thanks to the MUI-free reception, the BER remains unchanged when the number of active users $M_a (M_a \leq M)$ varies. However, for both DS-CDMA and MC-CDMA, when the number of active users M_a increases, the performance of each user degrades, as shown in Figs. 7(a)–(d). When the system is lightly loaded, i.e., $M_a \ll M$, the multiuser detectors could exhibit better performance since MUI is less severe in this case. When the system is moderately or heavily loaded, e.g., $M_a \approx M$, the proposed MUI-free transceiver outperforms the multiuser-detectors as confirmed by Fig. 7.

Test Case 2 (Comparison With the MUI-Free Transceiver of [15] and [16]): To compare the proposed transceiver with those in [15] and [16], we here adopt ZF equalizers and the design parameters of [15] for its shift-orthogonal transceiver: $L = 3$ (4-ray channels), $K = 4$ and $M_2 = 8$ users. The code length (spreading gain) for each user is then $N = 2M + 1 = 17$

⁷Fig. 7 also shows that DS-CDMA and MC-CDMA have quite different performance in the presence of multipath, as studied in [31].

⁸We used [28, eq. (23)] to evaluate the MMSE receiver performance.

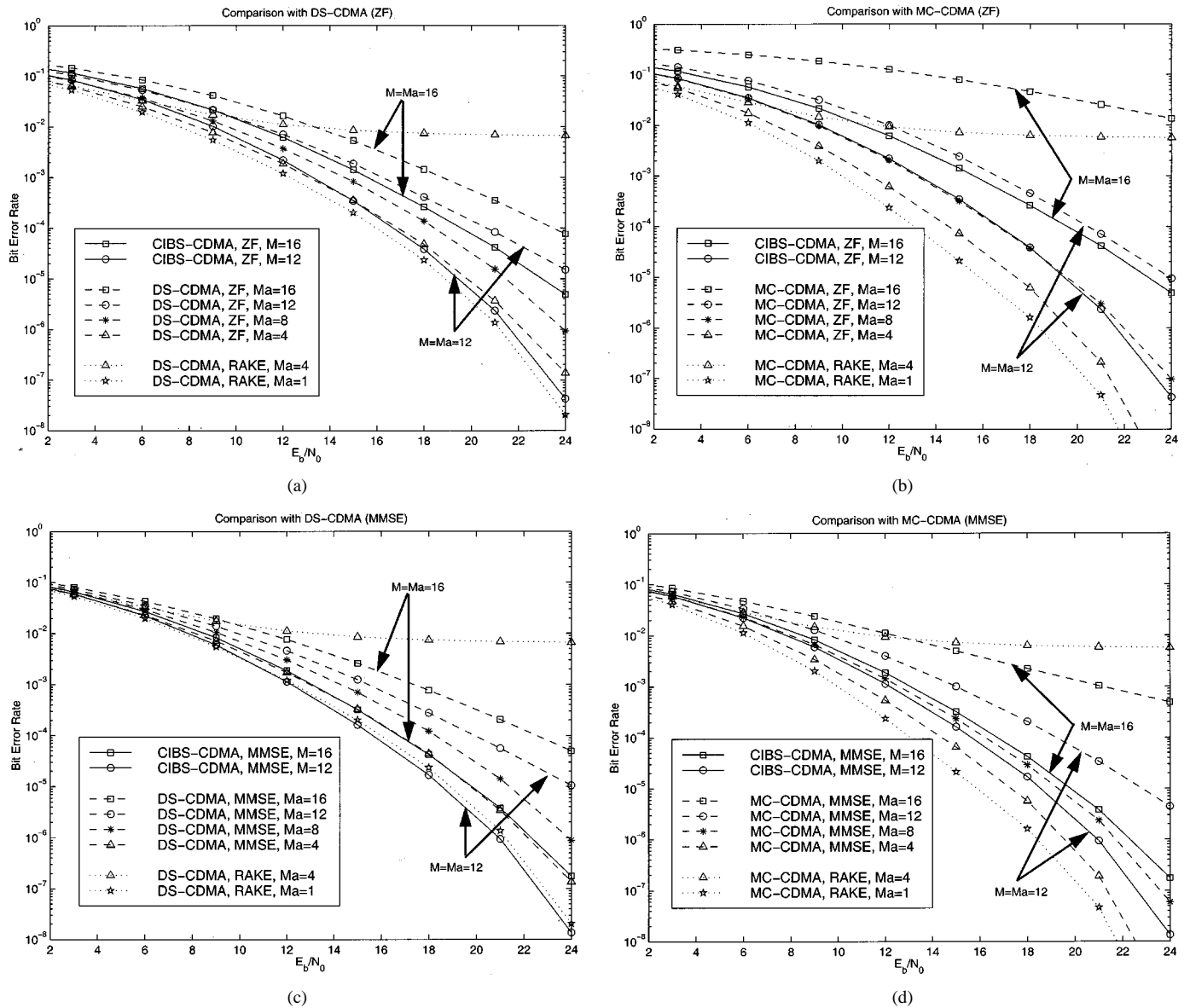


Fig. 7. Comparisons with multiuser detectors. (a) CIBS-CDMA versus DS-CDMA, ZF receiver. (b) CIBS-CDMA versus MC-CDMA, ZF receiver. (c) CIBS-CDMA versus DS-CDMA, MMSE receiver. (d) CIBS-CDMA versus MC-CDMA, MMSE receiver.

to satisfy the shift-orthogonality between user codes; the block length is thus $P_2 = NK = 68$.

Note that increasing K does not bring additional benefits to [15] and [16], while system decoding complexity and delays increase. However, K is very flexible in our system design and different tradeoffs can be exploited between decoding complexity/delay, BER performance, and bandwidth efficiency, which is determined by the maximum number of MUI-free users and the information rate of each user. To make a fair comparison, we put both transceivers with the same information rate R_b under the same system bandwidth W , and thus the same spreading gain $N = W/R_b = 17$. Various system designs can be afforded by the proposed transceiver as detailed in the following.

1) We fix our system to have the same decoding delay by adopting $K = 4$. Therefore, we can afford $M_1 = 9$ users [cf. (21)], and the block length becomes $P_1 = M_1(K + L) = 63$. Since $M_1 > M_2$ and $P_1 < P_2$, our system accommodates one

more user with shorter blocks, which implies that our system has higher bandwidth efficiency than [15]: $\mathcal{E}_1 = M_1K/P_1 > \mathcal{E}_2 = M_2K/P_2$. However, since both systems reach the same block model of (11), each user has the same performance as confirmed by Fig. 8 with $K = 4$. The only difference here is that the system of [15], [16] incurs a small power loss $10 \log_{10}(17/16) = 0.26$ dB due to the cyclic prefix of length 1 (out of $N = 17$) that is discarded at the receiver. Notice that additional power loss will occur in the proposed CIBS-CDMA if we fill the zero guards with known symbols to make up for perfect constant modulus.

2) As confirmed by (21), the number of users increases for fixed N when K increases. For example, with $K = 6, 8, 14$ we allow for 11, 12, 14 MUI-free users within a block of length $P_1 = 11 \times 9 = 99, 12 \times 11 = 132, 14 \times 17 = 238$, respectively. For FIR channels of maximum order L , a total of $N - 1$ users are allowed when $K = L(N - 1)$. In addition to larger decoding complexity/delays, the BER performance degrades, as shown in Fig. 8, as the maximum number of users increases.

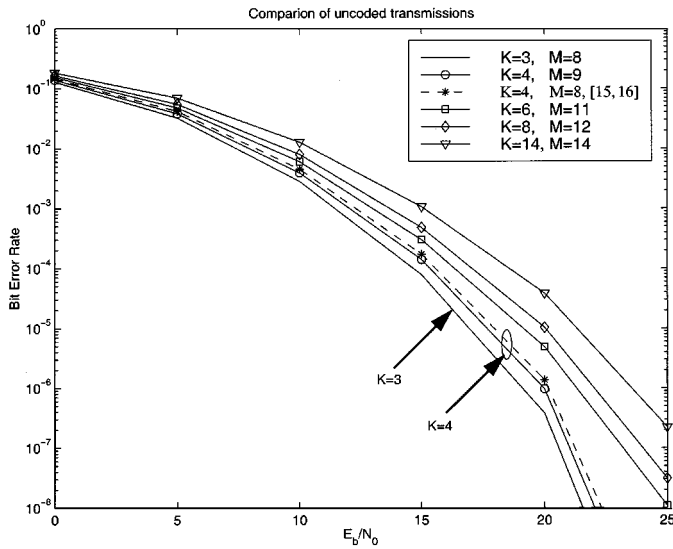


Fig. 8. BER comparison with [15] and [16].

Clearly, we see the trade-offs emerging among bandwidth efficiency, decoding complexity/delays and BER performance. We can also infer from Fig. 8 that increasing K in [15], [16] degrades system performance because it reaches the same model (11). However, the bandwidth efficiency does not improve with K , and is always limited to $MK/NK < 50\%$.

3) We now fix the number of users to $M_1 = M_2 = 8$. Then the block length K should be chosen to satisfy: $M_1(K + L) < KN$, which requires $K > LM_1/(N - M_1)$. Note that with $M_1 = M_2 = (N - 1)/2$, we can always choose the minimum $K = L$ since $M_1/(N - M_1) < 1$. Therefore, we can set $K = L = 3$ here and $P_1 = 8 \times 6 = 48$, which results in smaller decoding complexity/delays and leads to better BER performance, which is shown in Fig. 8 with $K = 3$. On the other hand, we can increase the number of symbols within each data vector $\mathbf{x}(i)$ to increase throughput for a fixed number of users. For example, with a block length $P_1 = 63, 72$, we can allow for $K = 5, 6 > 4$ symbols for each of the M_1 users. However, when K and hence the symbol rate per user increases, the BER performance degrades, which can be confirmed by Fig. 8. The reason is that when K increases, the spreading gain per symbol decreases: $P_1/K = M_1(K + L)/K$, and thus the system resources are not fully utilized. To fully exploit the system bandwidth resources $P_1/K \approx N$, we can for example transmit the linearly precoded or channel coded $K' \times 1$ vector $\mathbf{s}'_m(i)$ (e.g., as in (32)) instead of the $K \times 1$ data vector $\mathbf{s}_m(i)$. For example, within the spreading gain $N = 17$, we can set $(K', K) = (8, 6)$ or $(9, 6)$ for linear precoding or adopt channel coding with rate $6/8$ or $6/9$ to improve the BER performance. To illustrate this point, a simple simulation is provided next.

4) We here simulate $M_1 = M_2 = 6$ users in both systems. Since $N - 1$ should be a power of 2 and $N/2 > 6$ in [15] and [16], the code length is again $N = 17$. Here, with the same $K = 4$, and $N = 17$, we use $K' = 7$ and a $(7, 4)$ Hamming code to improve the BER performance, as confirmed by Fig. 9 where the coded BER is calculated through [3, eqs. (10.67) and (10.101)]. We could also compare the coded transmissions for both systems. However, to maintain the same bandwidth effi-

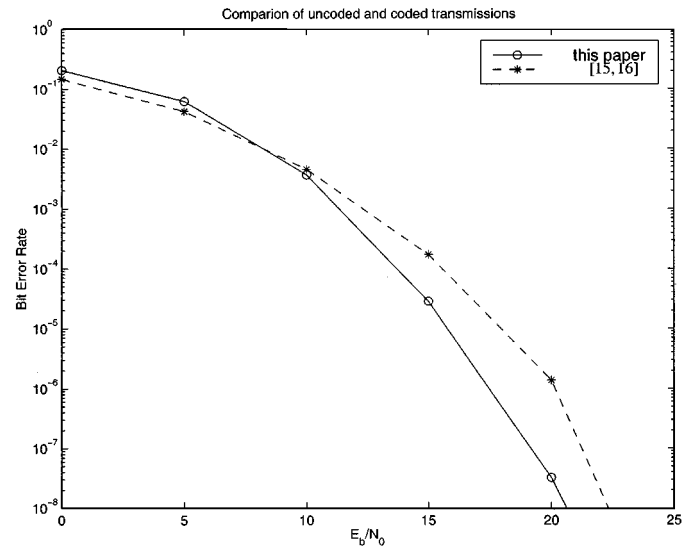


Fig. 9. Coding for a fixed number of users.

ciency, we need to adopt codes with different rates. Since low rate codes have stronger error-control capability, the comparison results would also favor the proposed CIBS-CDMA. For this reason, we just construct a simple artificial case here with Hamming codes to illustrate the point.

Test Case 3 (Comparison of (Semi-) Blind Channel Estimators): To test the blind channel estimators outlined in Section V, we here simulate a system having parameters: $K = 8, L = 3$, and equipped with ZF equalizers. However, to provide a very low-complexity channel estimator based on the FA property of the source symbols (cf. Section V-B), we also precode our transmission with a K -point IFFT as in (33) and choose to initialize the FA-based estimator with one training block. As noted in [24], the minimum number of data blocks needed to perform the subspace based method is $L + K = 11$. When only 15 blocks are collected, the FA-based channel estimator outperforms the subspace based alternative considerably as verified by Fig. 10, which also corroborates the fast convergence of the FA-based method. When more blocks become available, Fig. 11 illustrates that subspace based methods can also approach the benchmark theoretical performance of (35) with known channels. As mentioned in Section V and confirmed by Figs. 10 and 11, the drawback of subspace based methods is their slow convergence and high computational complexity. On the positive side, the subspace based method is constellation-independent, and thus it can be applied to any of the nonredundant precoded and loaded transmissions that we discussed in Section IV-C. In contrast, the FA-based channel estimator is tailored to the FFT precoded transmission in (33), to offer fast convergence and low complexity.

VII. CONCLUSION

A novel MUI-free CDMA transceiver was developed in this paper for frequency-selective multipath channels. Relying on chip (de-)interleaving and matched filtering operations only, a multiuser detection problem was converted into a set of equivalent single-user equalization problems without loss of ML optimality. In addition to MUI-free reception, symbols were also

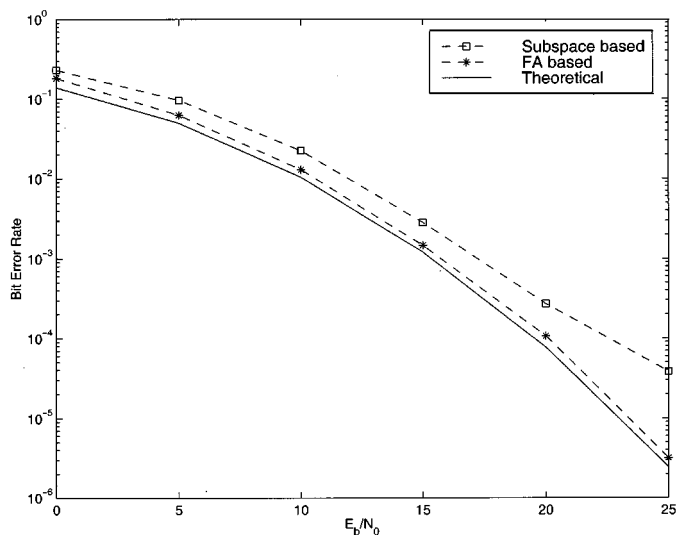


Fig. 10. Channel estimation with 15 blocks.

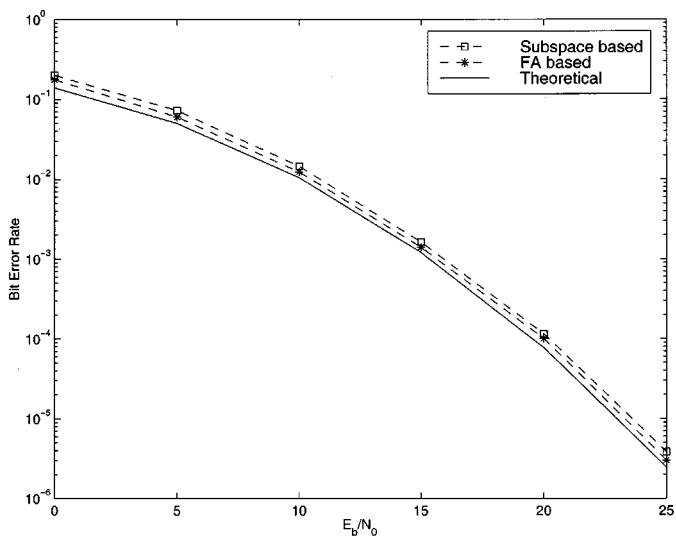


Fig. 11. Channel estimation with 30 blocks.

guaranteed to be detectable regardless of channel zero locations. By increasing the symbol block size, the proposed system achieves high bandwidth efficiency, and by filling the zero gaps with known symbols enables transmissions with perfectly constant modulus. Variants were also developed to include cyclic prefixed transmissions, and various redundant as well as nonredundant precoding alternatives. Separating the superposition of multiuser transmissions through frequency-selective multipath enabled application of single-user (semi-) blind channel estimation and equalization algorithms for intersymbol interference mitigation. Simulation results corroborated the improved performance relative to competing alternatives.

REFERENCES

[1] 3GPP-TSG-RAN-WG4; UTRA (BS) TDD; Radio Transmission and Reception (1999, Dec.). [Online]. Available: www.etsi.org/umts
 [2] T. Beer, "Walsh transforms," *Amer. J. Phys.*, vol. 49, no. 5, pp. 466–472, 1981.
 [3] S. Benedetto and E. Biglieri, *Principles of Digital Transmission with Wireless Applications*. Boston, MA: Kluwer, 1999.

[4] J. A. C. Bingham, "Multicarrier modulation for data transmission: An idea whose time has come," *IEEE Commun. Mag.*, pp. 5–14, May 1990.
 [5] J. W. Brewer, "Kronecker products and matrix calculus in system theory," *IEEE Trans. Circuits Syst.*, vol. CAS-25, pp. 772–781, Sept. 1978.
 [6] J. K. Cavers, "An analysis of pilot symbol assisted modulation for Rayleigh fading channels (mobile radio)," *IEEE Trans. Veh. Technol.*, vol. 40, pp. 686–693, Nov. 1991.
 [7] H. A. Cirpan and M. K. Tsatsanis, "Chip interleaving in direct sequence CDMA systems," in *Proc. Int. Conf. on ASSP*, vol. 5, 1997, pp. 3877–3880.
 [8] M. V. Clark, "Adaptive frequency-domain equalization and diversity combining for broadband wireless communications," *IEEE J. Select. Areas Commun.*, vol. 16, pp. 1385–1395, Oct. 1998.
 [9] G. D. Forney Jr., "Maximum-likelihood sequence estimation of digital sequences in the presence of intersymbol interference," *IEEE Trans. Inform. Theory*, vol. IT-18, pp. 363–378, May 1972.
 [10] G. B. Giannakis, P. Anghel, and Z. Wang, "Wideband generalized multi-carrier CDMA over frequency-selective wireless channels," *Proc. ICASSP*, vol. 5, pp. 2501–2504, 2000.
 [11] G. B. Giannakis, Z. Wang, A. Scaglione, and S. Barbarossa, "AMOUR—Generalized multi-carrier transceivers for blind CDMA regardless of multipath," *IEEE Trans. Commun.*, vol. 48, pp. 2064–2076, Dec. 2000.
 [12] S. W. Golomb and L. D. Baumert, "The search for Hadamard matrices," *Amer. Math. Monthly*, vol. 70, no. 1, pp. 12–17, Jan. 1963.
 [13] G. H. Golub and C. F. Van Loan, *Matrix Computations*, 3rd ed. Baltimore, MD: Johns Hopkins Univ. Press, 1996.
 [14] W. M. Jang, B. R. Vojčić, and R. L. Pickholtz, "Joint transmitter-receiver optimization in synchronous multiuser communications over multipath channels," *IEEE Trans. Commun.*, vol. 46, pp. 269–278, Feb. 1998.
 [15] G. Leus and M. Moonen, "MUI-free receiver for a shift-orthogonal quasisynchronous DS-SS-CDMA system based on block spreading in frequency-selective fading," in *Proc. Int. Conf. ASSP*, Istanbul, Turkey, June 5–9, 2000, pp. 2497–2500.
 [16] —, "MUI-free receiver for a synchronous DS-SS-CDMA system based on block spreading in the presence of frequency-selective fading," *IEEE Trans. Signal Processing*, vol. 48, pp. 3175–3188, Nov. 2000.
 [17] H. Liu and G. Xu, "A subspace method for signature waveform estimation in synchronous CDMA systems," *IEEE Trans. Commun.*, vol. 44, pp. 1346–1354, Oct. 1996.
 [18] B. Muquet, M. de Courville, P. Duhamel, and V. Bueñac, "A subspace based blind and semi-blind channel identification method for OFDM systems," in *Proc. SPAWC*, Annapolis, MD, May 9–12, 1999, pp. 170–173.
 [19] B. Muquet, Z. Wang, G. B. Giannakis, M. de Courville, and P. Duhamel, "Cyclic prefix or zero-padding for multi-carrier transmissions?," *IEEE Trans. Commun.*, to be published.
 [20] S. P. Reichhart, B. Youmans, and R. Dygert, "The software radio development system," *IEEE Personal Commun.*, vol. 6, pp. 20–24, Aug. 1999.
 [21] A. Ruiz, J. M. Cioffi, and S. Kasturia, "Discrete multiple tone modulation with coset coding for the spectrally shaped channel," *IEEE Trans. Commun.*, vol. 40, pp. 1012–1029, June 1992.
 [22] H. Sari and G. Karam, "Orthogonal frequency-division multiple access and its application to CATV network," *Eur. Trans. Telecommun.*, vol. 9, pp. 507–516, Nov./Dec. 1998.
 [23] H. Sari, G. Karam, and I. Jeanclaude, "Transmission techniques for digital terrestrial TV broadcasting," *IEEE Commun. Mag.*, vol. 33, pp. 100–109, Feb. 1995.
 [24] A. Scaglione, G. B. Giannakis, and S. Barbarossa, "Redundant filterbank precoders and equalizers: Part I & Part II," *IEEE Trans. Signal Processing*, vol. 47, pp. 1988–2022, July 1999.
 [25] —, "Lagrange/Vandermonde MUI eliminating user codes for quasisynchronous CDMA in unknown multipath," *IEEE Trans. Signal Processing*, vol. 48, pp. 2057–2073, July 2000.
 [26] S. Verdú, *Multiuser Detection*. Cambridge, U.K.: Cambridge Univ. Press, 1998.
 [27] Z. Wang and G. B. Giannakis, "Wireless multicarrier communications: Where Fourier meets Shannon," *IEEE Signal Processing Mag.*, pp. 29–48, May 2000.
 [28] —, "Block-precoding for MUI/ISI-resilient generalized multi-carrier CDMA with multirate capabilities," *IEEE Trans. Commun.*, vol. 49, 2001.
 [29] G. Q. Xue, J. E. Weng, T. Le-Ngoc, and S. Tahar, "Impact of imperfect power control and channel estimation on the performance of multiuser detectors," in *Proc. Global Telecommunications Conf.*, vol. 1, 1999, pp. 138–142.

- [30] S. Zhou and G. B. Giannakis, "Finite-alphabet based channel estimation for OFDM and related multi-carrier systems," *IEEE Trans. Commun.*, vol. 49, pp. 1402–1414, Aug. 2001.
- [31] S. Zhou, G. B. Giannakis, and A. Swami, "Comparison of digital multi-carrier spread spectrum and direct sequence spread spectrum in the presence of multipath," in *Proc. ICASSP*, Salt Lake City, UT, May 7–11, 2001.



Shengli Zhou (S'99) was born in Anhui, China, in 1974. He received the B.S. and M.Sc. degrees in electrical engineering and information science from the University of Science and Technology of China (USTC), China, in 1995 and 1998, respectively. He is currently working toward the Ph.D. degree in the Department of Electrical and Computer Engineering at the University of Minnesota, Minneapolis.

His broad interests lie in the areas of communications and signal processing, including transceiver optimization, blind channel estimation and equalization

algorithms, and wireless, multi-carrier, space-time coded and spread-spectrum communication systems.



Georgios B. Giannakis (S'84–M'86–SM'91–F'97) received the Diploma in electrical engineering from the National Technical University of Athens, Athens, Greece, in 1981. From September 1982 to July 1986, he was with the University of Southern California (USC), Los Angeles, where he received the M.Sc. degree in electrical engineering in 1983, the M.Sc. degree in mathematics in 1986, and the Ph.D. degree in electrical engineering, in 1986.

After lecturing for one year at USC, he joined the University of Virginia, Charlottesville, in 1987,

where he became a Professor of electrical engineering in 1997. Since 1999, he has been a Professor with the Department of Electrical and Computer Engineering with the University of Minnesota, Minneapolis, where he now holds an ADC Chair in wireless telecommunications. His general interests span the areas of communications and signal processing, estimation and detection theory, time-series analysis, and system identification—subjects on which he has published more than 140 journal papers, 270 conference papers, and two edited books. Current research topics focus on transmitter and receiver diversity techniques for single- and multi-user fading communication channels, precoding and space-time coding for block transmissions, multicarrier, and wide-band wireless communication systems. He is a frequent consultant to the telecommunications industry.

Dr. Giannakis is the co-recipient of four best paper awards from the IEEE Signal Processing (SP) Society (1992, 1998, 2000, and 2001). He also received the SP Society's Technical Achievement Award in 2000. He co-organized three IEEE Signal Processing Workshops, and guest co-edited four special issues. He has served as Editor-in-Chief for the *IEEE SIGNAL PROCESSING LETTERS*, Associate Editor for the *IEEE TRANSACTIONS ON SIGNAL PROCESSING*, and the *IEEE SIGNAL PROCESSING LETTERS*, secretary of the Signal Processing Conference Board, member of the Signal Processing Publications Board, member and vice-chair of the Statistical Signal and Array Processing Technical Committee, and as chair of the Signal Processing for Communications Technical Committee. He is a member of the Editorial Board for the *PROCEEDINGS OF THE IEEE*, and the steering committee of the *IEEE TRANSACTIONS ON WIRELESS COMMUNICATIONS*. He is a member of the IEEE Fellows Election Committee, and the IEEE Signal Processing Society's Board of Governors.



Christophe Le Martret was born in Rennes, France, on March 12, 1963. He received the Ph.D. degree from l'Université de Rennes 1, Rennes, France, in 1990.

From 1991 to 1995 he was with the CESTA, Bruz, France, and has been with the Centre d'Électronique de L'Armement (CELAR) since 1996. He was a Visiting Researcher at the SpinCom Laboratory, Department of Electrical and Computer Engineering, University of Minnesota, Minneapolis, from 1999 to 2000. He has been teaching digital communications at École d'Ingénieurs Louis de Broglie, Bruz, France, since 1998. His current research interests are in statistical signal processing and communications: modulation classification, equalization, multi-user detection, and ultrawide-band communications.